SCIENTIFIC REPORTS

OPEN

SUBJECT AREAS:
MAGNETIC PROPERTIES AND MATERIALS
FERROELECTRICS AND MULTIFERROICS
PHASE TRANSITIONS AND CRITICAL PHENOMENA

Received
6 May 2014

Accepted
30 October 2014

Published
17 November 2014

Correspondence and requests for materials should be addressed to J.W. (wangjing@iphy.ac.cn) or F.-X.H. (fxhu@iphy.ac.cn)

Abnormal percolative transport and colossal electroresistance induced by anisotropic strain in (011)-$Pr_{0.7}(Ca_{0.6}Sr_{0.4})_{0.3}MnO_3$/PMN-PT heterostructure

Ying-Ying Zhao, Jing Wang, Hao Kuang, Feng-Xia Hu, Hong-Rui Zhang, Yao Liu, Ying Zhang, Shuan-Hu Wang, Rong-Rong Wu, Ming Zhang, Li-Fu Bao, Ji-Rong Sun & Bao-Gen Shen

Beijing National Laboratory for Condensed Matter Physics and State Key Laboratory of Magnetism, Institute of Physics, Chinese Academy of Sciences, Beijing 100190, P. R. China.

Abnormal percolative transport in inhomogeneous systems has drawn increasing interests due to its deviation from the conventional percolation picture. However, its nature is still ambiguous partly due to the difficulty in obtaining controllable abnormal percolative transport behaviors. Here, we report the first observation of electric-field-controlled abnormal percolative transport in (011)-$Pr_{0.7}(Ca_{0.6}Sr_{0.4})_{0.3}MnO_3$/$0.7Pb(Mg_{1/3}Nb_{2/3})O_3$-$0.3PbTiO_3$ heterostructure. By introducing an electric-field-induced in-plane anisotropic strain-field in a phase separated PCSMO film, we stimulate a significant inverse thermal hysteresis (~ -17.5 K) and positive colossal electroresistance (~11460%), which is found to be crucially orientation-dependent and completely inconsistent with the well accepted conventional percolation picture. Further investigations reveal that such abnormal inverse hysteresis is strongly related to the preferential formation of ferromagnetic metallic domains caused by in-plane anisotropic strain-field. Meanwhile, it is found that the positive colossal electroresistance should be ascribed to the coactions between the anisotropic strain and the polarization effect from the poling of the substrate which leads to orientation and bias-polarity dependencies for the colossal electroresistance. This work unambiguously evidences the indispensable role of the anisotropic strain-field in driving the abnormal percolative transport and provides a new perspective for well understanding the percolation mechanism in inhomogeneous systems.

In perovskite manganites $R_{1-x}A_xMnO_3$ (R and A being trivalent and divalent cations), the strong spin-charge-lattice coupling often leads to an electronic inhomogeneity called electronic phase separation (EPS), which is usually identified with the coexistence of ferromagnetic metal (FMM) and charge-ordered insulator (COI)[1]. Direct imaging results have been brought forth, revealing mesoscopic ferromagnetic (FM) clusters inside an antiferromagnetic (AFM)/COI matrix[2,3]. There are growing experimental evidences that the coexistence and competition of FMM and COI phases lead to percolation-driven insulator-metal transition (IMT) accompanied by a obvious thermal hysteresis due to the first order nature of the transition[4–10]. Typically, in the vicinity of the transition, the resistivity of the percolation-driven manganites usually tends to retain the high temperature (or low temperature) value when the temperature is decreased (or increased), resulting in a normal hysteresis[7,11]. However, with increasing temperature from the low temperature region where the FMM phase predominates, an abnormal effect of "overshot" hysteresis was occasionally observed in few charge-ordered manganites including $Sm_{0.65}Sr_{0.35}MnO_3$ (ref. 12), and $Pr_{0.5}Ca_{0.5}(Mn,Cr)O_3$ (ref. 13). Moreover, K. De *et al.*[14] observed a complete inverse thermal hysteresis of ~−5 K in polycrystalline self-doped $La_{0.87}Mn_{0.98}Fe_{0.02}O_x$ under magnetic-field-cooling condition. Markovich *et al.*[15] reported a small inverse hysteresis narrower than −3.5 K in self-doped $La_{0.9}MnO_{3-\delta}$ film, independent of the external magnetic field. Such abnormal inverse thermal hysteresis is inconsistent with the well accepted conventional percolation picture and deserves careful investigations due to the key role of the percolative manner in accurately understanding the magnetic and electric properties of phase separation systems.

Khomskii *et al.*[16] once proposed a modified percolation scenario to explain such abnormal percolative transport behaviors by assuming a different distribution of FM clusters in size and shape during decreasing and increasing temperature. In this scenario, a lot of small metallic clusters are proposed to appear in the sample while decreasing temperature, whereas much fewer numbers of large metallic clusters with big insulator barriers between them emerge with increasing temperature. Therefore, the resistivity on increasing temperature will be larger than the one on decreasing temperature, thus resulting in an inverse hysteresis. By using Monte Carlo method, Khomskii *et al.* further simulated the formation process of metal clusters. They found that the aforementioned physical picture, *i.e.* different distributions of FM clusters for decreasing and increasing temperature, would be well reproduced while taking into account the correlated occupation of metallic sites in the simulation[16]. However, a convincing explanation of the correlated occupation of the metallic sites, especially its original driving force is still lack, which makes the nature of the abnormal percolative transport behaviors keep ambiguous. Moreover, detailed experimental investigations of the abnormal percolative transports are absent up to now, which is partly due to the difficulty in obtaining a controllable inverse hysteresis in EPS systems. Previous theoretical[6,11,17,18] and experimental[19–21] investigations have revealed that the elastic distortion due to Jahn-Teller coupling plays an important role in affecting the EPS,especially the distribution of separated phases. Moreover, studies showed that the large-scale EPS can self-organize into elongated FM domains along the direction with higher-tensile-strain-field[6,11,22]. Naturally, one would associate the lattice strain-field with the correlated occupation of metallic sites. If a strong enough strain-field is applied to the system with a moderate phase competition, preferential formation of the clusters, *i.e.* correlated occupation of the metallic sites, may be expected. Thus considerable abnormal percolative transport might appear in such moderately phase-separated systems.

Following this idea, we investigate the transport behaviors under external electric field in phase separated (011)-$Pr_{0.7}(Ca_{0.6}Sr_{0.4})_{0.3}MnO_3$(PCSMO)/0.7$Pb(Mg_{1/3}Nb_{2/3})O_3-0.3PbTiO_3$(PMN-PT) heterostructure. The thin film of PCSMO is used as model system owing to its well-known large-scale EPS and moderate competition of two phases due to the substitution of Sr^{2+} for Ca^{2+} (ref. 23). Meanwhile, the single crystal of PMN-PT is chosen as substrate due to its excellent piezoelectric effect. The lattice strain and thus the electronic and magnetic properties of the manganite film on the PMN-PT can be easily controlled by tuning the electric field applied on the substrate[24–26]. Specially, with the electric field normal to the (011) plane, the (011)-cut PMN-PT single crystal slab shows a large anisotropic piezoelectric effect[27], which provides an exceptional opportunity for dynamically generating a large in-plane anisotropic strain in the film epitaxially grown on it. It is conceivable that such electric-field induced anisotropic strain will stimulate the preferential formation of clusters/domains and promote the appearance of abnormal percolative behaviors. Actually, we do observe a considerable inverse thermal hysteresis (~ -17.5 K and -8.5 K under an electric field of $+10$ kV/cm and -10 kV/cm, respectively) in the PCSMO/PMN-PT heterostructure. It is demonstrated that the preferential formation of FMM domains caused by anisotropic strain-field fulfills the requirement of correlated occupation of the metal sites, resulting in a different distribution of domains for decreasing and increasing temperature processes, and thus stimulates a abnormal inverse hysteresis. Moreover, the preferential formation also induces different topological structures of FMM and COO insulating phases along [100] and [01$\bar{1}$] directions, and thus results in an orientation dependence of the abnormal percolative transport. Meanwhile, the resistance of the film was modulated by the polarization effect from the poling of PMN-PT. As a result, the resistivity in heating process exhibits a dramatic increase under the application of external electric-field due to the joint effect of the large anisotropic strain and polarization effect on the EPS, leading to an orientation and polarity-dependent positive colossal electroresistance ($\sim$11460% at in-plane [100] direction). Furthermore, we find that an external magnetic field can make the normal thermal hysteresis in the [01$\bar{1}$] direction change to an inverse one. Meanwhile, the [100] direction behaves opposite. These surprising results unambiguously evidence the crucial role of the anisotropic strain-field induced preferential formation of domains in driving the correlated occupation of metallic sites and thus the abnormal percolative behaviors in EPS systems.

Results

The heterostructure composed of 100 nm PCSMO film and (011)-oriented PMN-PT was prepared by using pulsed laser deposition (PLD). Sample configuration is shown in the inset of Fig. 1(a). The XRD θ-2θ scan for the (011)-PCSMO/PMN-PT heterostructure shows that the film is fully textured with out-of-plane direction [011] and no other phases or textures are observed, as shown in Fig. 1(a). The out-of-plane lattice constant for 100 nm (011)-PCSMO/PMN-PT film is determined to be 2.720 Å. Thus, the corresponding out-of-plane strain is calculated to be -0.26% by using $\varepsilon_{011} = (d_{film}-d_{bulk})/d_{bulk}$, indicating the film undergoes compressive strain along the out-of-plane direction. To obtain the in-plane epitaxial strain along in-plane orthogonal [100] and [01$\bar{1}$] directions, x-ray reciprocal space maps (RSMs) around (222) and (013) reflections were collected, as shown in Fig. 1(c) and (d). The extracted in-plane lattice constants of d_{100} and $d_{01\text{-}1}$ for the 100 nm film are determined to be 3.876 Å and 2.738 Å, respectively, which is a bit larger than those of bulk (3.858 and 2.727 Å). Thus, the corresponding in-plane strains are tensile ones, e.g. 0.47% and 0.40% for [100] and [01$\bar{1}$] directions, respectively. Due to the excellent anisotropic piezoelectric effect of (011)-cut PMN-PT, applying an external electric field parallel to the [011] direction would induce a sizable anisotropic in-plane strain in the PMN-PT crystal, which could be directly transformed to the PCSMO film grown on it[28,29]. Fig. 1(b) displays the field-induced in-plane strain ε_{100} and $\varepsilon_{01\text{-}1}$ in PCSMO film as a function of the bipolar bias electric field on PMN-PT substrate at 300 K. It is seen that a significant compressive strain (~ -0.31%) along in-plane [100] and a very small tensile one ($\sim$0.018%) along in-plane [01$\bar{1}$] appear concurrently in the sample while the bipolar bias field on PMN-PT reaches 6 KV/cm. It is noted that the electric field-induced compressive strain along [100] is larger than the biaxial strain in most films on (001)-cut PMN-PT[24–25,28,30–32]. Such large anisotropic in-plane strain may cause sizable anisotropic response in the EPS and percolative transport behaviors of PCSMO system.

Figure 2 plots the temperature dependence of resistance (R-T) for bulk and the PCSMO film along two in-plane directions under no electric field. The bulk sample shows an insulator-metal transition (IMT) around $T_{IMT}\sim 175$ K (defined as the peak temperature in R-T curves on heating) with a normal thermal hysteresis ($\Delta T\sim 3.5$ K, see Fig. 2(a)) on the left side of the peak. Such normal hysteresis behavior is consistent with previous report and the conventional percolation feature, indicating a coexistence of separated COI and FMM phases and percolation transport[7,23]. Compared to the typical EPS systems, such as $La_{5/8\text{-}y}Pr_yCa_{3/8}MnO_3$ (ref. 7), the hysteresis gap of present PCSMO is narrower, which may suggest a moderate competition between COI and FMM phases. Furthermore, one can find that the film of PCSMO on (011)-PMN-PT in the absence of external field remains bulk's percolative transport behavior, *i.e.* the normal thermal hysteresis at both perpendicular in-plane directions (Fig. 2(b) and (c)). The transition temperature T_{IMT} and the hysteresis gap ΔT are found to be 121.5 K, 4.5 K and 124 K, 5 K, for [100] and [01$\bar{1}$] directions, respectively. The decrease in transition temperature, T_{IMT}, and widening of the hysteresis gap compared to the bulk should be ascribed to the in-plane epitaxial tensile strain[21,33]. Meanwhile, a clear EPS was observed around the transition temperature ($T_{IMT}\sim 121.5$ K and 124 K for [100] and [01-1] directions,

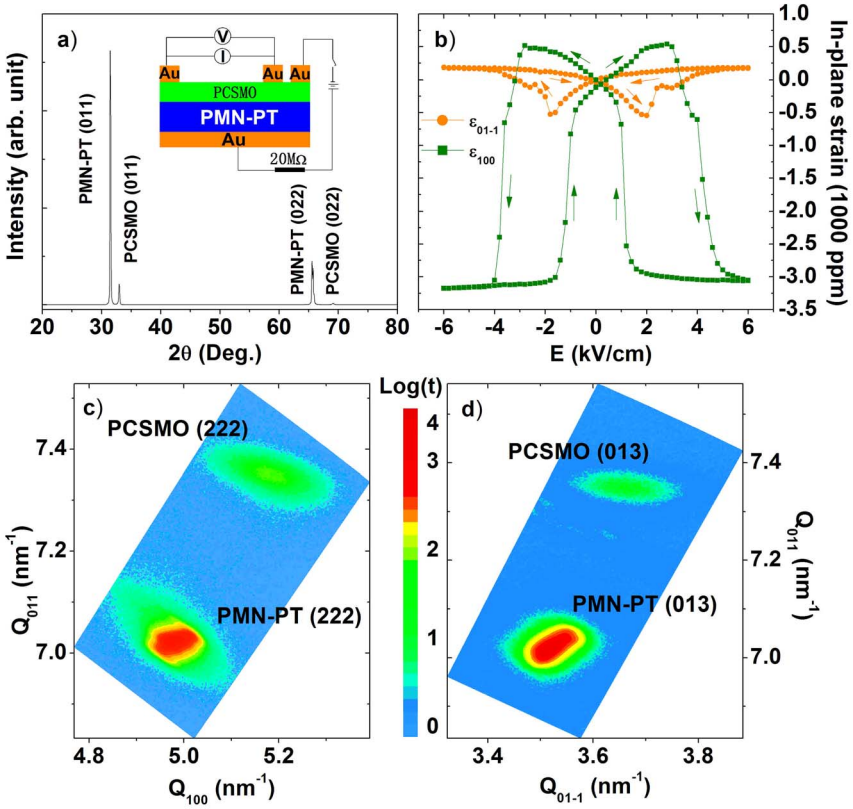

Figure 1 | (a) X-ray diffraction patterns of the PCSMO/PMN-PT heterostructure. The inset is the schematic diagram of measurement circuit for the heterostructure. (b) In-plane strain ε_{100} and $\varepsilon_{01\text{-}1}$ of PCSMO film vs. E at 300 K, the arrows indicate the directions of sweeping E. (c) and (d) X-ray reciprocal space maps around (222) and (013) reflections for the heterostructure, respectively.

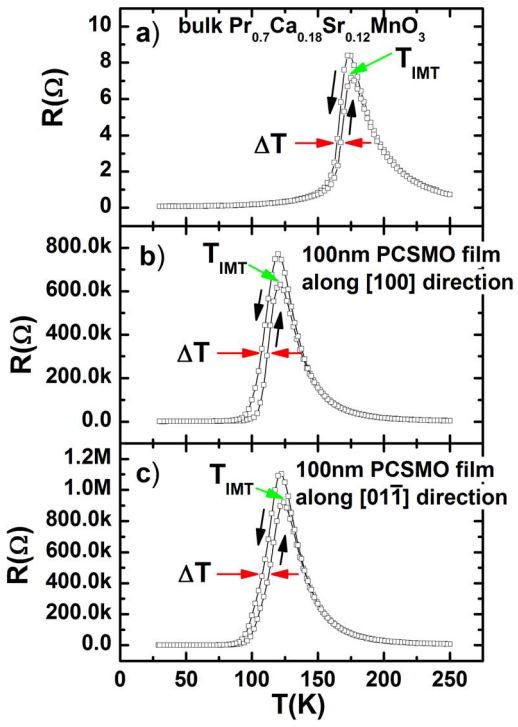

Figure 2 | **Temperature dependent resistance of (a) bulk $Pr_{0.7}(Ca_{0.6}Sr_{0.4})_{0.3}MnO_3$, 100 nm (011)-PCSMO/PMN-PT film along in-plane (b) [100] direction and (c) [01$\bar{1}$] directions.** The black arrows indicate the directions of temperature sweeping while red arrows denote the hysteresis gap ΔT.

respectively) by Lorentz transmission electron microscopy. Such EPS regions were further found to vary with the temperature, in coincidence with the transport results (detailed discussions see section S1 in supplementary material).

Upon application of bias electric-field of ±10 kV/cm, the percolative behavior of the film, especially in the in-plane [100] direction, exhibits novel changes. First of all, with applying an electric field of +10 kV/cm on the PMN-PT substrate, the IMT temperature (T_{IMT}, the peak temperature on heating as defined above) along the [100] direction shows a shift about ~14 K towards lower temperature (Fig. 3(a)). More importantly, the resistance measured along the [100] direction dramatically increases in the heating branch while slightly decreases in the cooling branch around T_{IMT}. Such a response of the resistance to the electric bias field causes the heating branch rises to exceed the cooling one, resulting in novel phenomena: inverse thermal hysteresis and positive colossal electroresistance. It is determined, from the curves in Fig. 3(a), that the thermal hysteresis of the film in the direction of [100] changes from 4.5 K to −17.5 K (indicated by red arrows) as +10 kV/cm electric field is applied. Such abnormal inverse thermal hysteresis cannot be explained solely by conventional percolation picture, which predicts a normal hysteresis between the cooling and heating branches. To further quantify the influence of the electric field on percolative transport, we calculate the electroresistance, $\Delta R/R=(R(E)-R(0))/R(0)$, along two in-plane directions, as shown in Fig. 4(a) and (b). It is found that, with the application of bias field +10 kV/cm, the positive electroresistance along the in-plane [100] direction reaches a maximum of ~11460% at 95 K in the heating process (see Fig. 4(a)). To the best of our knowledge, such positive colossal electroresistance is firstly reported in the phase-separated manganite systems. The value exceeds that of most manganite systems previously reported. It was reported that, for a ferroelectric field effect transistor structure of

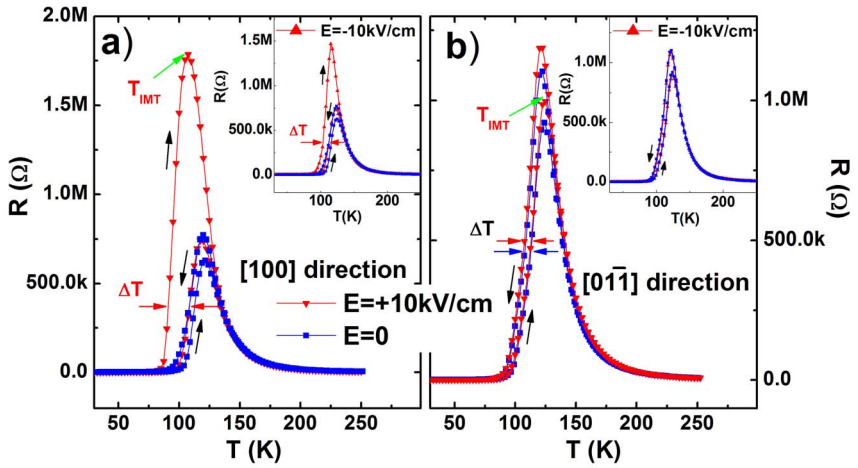

Figure 3 | Temperature dependent electric resistance of (011)-$Pr_{0.7}(Ca_{0.6}Sr_{0.4})_{0.3}MnO_3$/PMN-PT measured under bias field of 0 and +10 kV/cm for in-plane (a) [100] and (b) [01$\bar{1}$] directions. The inset presents the resistance under bias field of 0 and −10 kV/cm for corresponding directions. The black arrows indicate the directions of temperature sweeping while red and blue ones denote the hysteresis gap ΔT.

$La_{0.8}Ca_{0.2}MnO_3$-$Pb(Zr_{0.2}Ti_{0.8})O_3$, a maximal resistive modulation could reach +20% with a large electric field of +150 KV/cm at room temperature due to the field-induced polarization effect[26]. By using field-induced strain effect in (001)-$La_{0.7}Sr_{0.3}MnO_3$/$Pb(Mg_{1/3}Nb_{2/3})O_3$-$PbTiO_3$ structure, C. Thiele *et al.*[25] observed a negative electroresistance up to −9% at 300 K for a in-plane contraction of 0.1% induced by a electric field of 12.5 kV/cm. More recently, by combining the field-induced polarization and strain effect, Tao Jiang *et al.*[24] obtained a negative resistive modulation of −53.2% with E = 12 kV/cm at 140 K in $La_{0.7}Ca_{0.3}MnO_3$/$SrTiO_3$/$Pb(Mg_{1/3}Nb_{2/3})O_3$-$PbTiO_3$. In present work, the observed positive colossal electroresistance and different temperature dependency of the electroresistance in cooling and heating branches (see Fig. 4(a)) suggest that the electric field may have a different influence on the topological structure of coexisting phases in the [100] direction during cooling and heating processes, considering that the COI phase has a much higher resistivity than the FMM one. Moreover, experiments with a negative bias field of −10 kV/cm was also performed. Similar inverse hysteresis ΔT and positive colossal electroresistance ΔR/R are observed for the in-plane [100] direction (see the insets of Fig. 3(a) and 4(a)), suggesting that the electric-field-induced strain field may play a critical role in driving the abnormal percolative transport behaviors. The only differences from the case with applying positive bias are that the ΔT width (∼ −8.5 K) and ΔR/R magnitude (∼2130%) becomes smaller, indicating that polarization effect also affect the electric transport.

On the other hand, the transport along the in-plane [01$\bar{1}$] direction exhibits quite different behaviors from the one along the in-plane [100] direction, as shown in Fig. 3(b) and Fig. 4(b). No inverse thermal hysteresis is observed in the curves along the [01$\bar{1}$] direction, independent of the bias polarity (see Fig. 3(b) and its inset). Instead, the IMT temperature and the normal hysteresis gap along [01$\bar{1}$] keep almost unchanged compared to the case without electric fields. Applying positive electric field of +10 kV/cm causes the resistance increase modestly for both cooling and heating processes. Although the resulted electroresistance is still positive under +10 kV/cm, the maximum is only ∼71% and ∼16% at 95 K for the heating and cooling branches, respectively. For the case of applying a negative bias of −10 kV/cm, the electroresistance in the [01$\bar{1}$] direction (see the inset of Fig. 4(b)) is further getting smaller and even becomes negative, *i.e.* the maximum is 1.7% and the minimum is −32% at 92.5 K for the heating and cooling processes, respectively. The absence of inverse hysteresis and colossal electroresistance for the

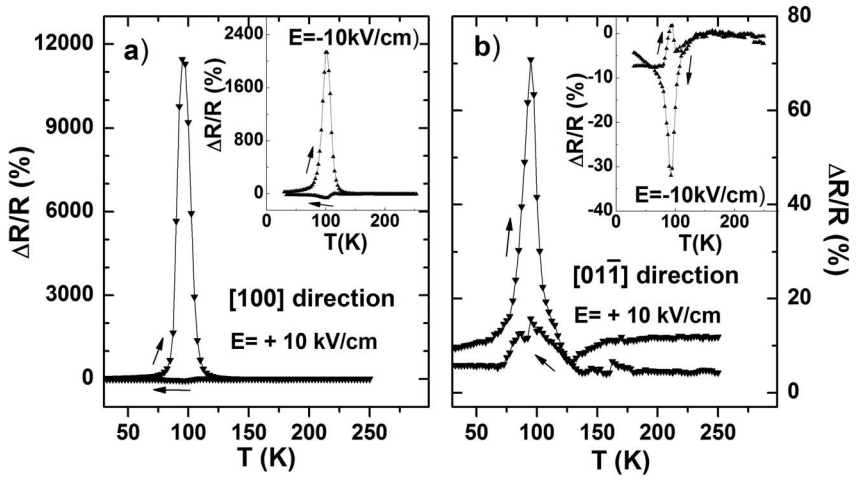

Figure 4 | The temperature dependent electroresistance, ΔR/R=(R(E)-R(0))/R(0), under a bias of +10 kV/cm along in-plane (a) [100] and (b) [01$\bar{1}$] directions. The insets plot the results under a negative bias of −10 kV/cm for corresponding directions. The arrows indicate the directions of sweeping temperature.

in-plane [01$\bar{1}$] direction indicates the vital role of the electric-field-induced in-plane anisotropic strain-field in stimulating the abnormal percolative transport behaviors.

Discussion

In a standard percolation scenario for the EPS system, the EPS features during cooling and heating processes are different. With decreasing temperature, FMM domains appear in a COI insulating matrix around the insulator-metal transition temperature, T_{IMT}. Further decreasing temperature causes the FMM domains develop and coalesce, and a percolation threshold is reached, characterized by a sudden drop of resistance. Finally, the whole sample is almost occupied by the FMM phase at low temperatures. However, in the heating process, COI droplets emerge and grow in the FMM matrix. These processes will be accompanied by a normal hysteresis if no external perturbation is applied. This hysteresis behavior is consistent with the first-order nature of the insulator-metal transition and appears in most percolation-driven phase-separated manganites including the bulk PCSMO[7,23,34] and (011)-PCSMO/PMN-PT film under no electric field (see Fig. 2). It's clear that the unusual effect of inverse hysteresis in present work cannot be explained by the standard percolation picture. Considering that the appearance of inverse hysteresis and positive colossal electroresistance are orientation-dependent, one may naturally associate it with the in-plane anisotropic strain-field caused by the electric-field bias.

Actually, previous works have demonstrated that in-plane strain can lead to local lattice distortions and strongly affects the formation of EPS[6,18,19,21]. Especially, studies based on the lattice degrees of freedom and the effects of electron-lattice coupling have shown that the large-scale EPS can self-organize into elongated domains along the direction with higher-tensile-strain-field[11,22]. The as-grown PCSMO film on PMN-PT substrate undergoes close tensile strains of 0.47% and 0.40% for the two in-plane orthogonal directions, i.e. [100], [01$\bar{1}$]. However, an electric bias of 6 kV/cm along the [011] direction of PMN-PT can cause a large compressive strain ($\sim -0.31\%$) along the [100] direction and a small tensile one (0.018%) along the [01$\bar{1}$] direction (see Fig. 1(b)). The introduced dynamic anisotropic strain-field will greatly reduce the epitaxial tensile strain in the film at [100] direction and slightly increase the one at [01$\bar{1}$] direction, resulting in a strong anisotropic tensile-strain-field along two in-plane directions: $\sim$0.16% for [100] and $\sim$0.42% for [01$\bar{1}$]. Thus, it will provide a driving force for correlated occupation of metallic sites and induce preferential formation of elongated FMM clusters along [01$\bar{1}$] since the film undergoes much higher tensile strain along [01$\bar{1}$] than along the [100] direction[11,22]. Meanwhile, the anisotropic strain-field would lead to a considerable but specific in-plane distortion of MnO_6 octahedron depending on the strain-state, which is significantly different from the effect induced by isotropic strain-field. As a result, the topological structure of orbital ordering for the two in-plane directions, which dominates transport behavior, would be drastically altered since 3d orbitals of Mn ions have been highly affected by the distortion. Along the [100] direction with specific topological structures of the EPS, many small FMM clusters may appear with decreasing temperature, whereas much fewer numbers of large FMM clusters with big insulator barriers between them may emerge with increasing temperature, according to the modified percolation model by Khomskii *et al.*[16]. Figure 5(a) and (b) present illustrations of how elongated domains act to transport current for cooling and heating processes, respectively. It is evident that the resistivity of the film for the [100] direction during the cooling process will be considerably smaller than the one during the heating process since the transport channel in the latter case has to cross over a bigger insulator barrier than the former case (see Fig. 5). As a result, an inverse hysteresis appears naturally in the [100] direction of our PCSMO film, as seen in Fig. 3(a). Moreover, with application of the external electric field, the current channel along [100] direction has to travel across more insulating regions than the one along [01$\bar{1}$] direction, as illustrated by red and yellow dotted lines and arrows in Fig. 5(a) and (b). This should be ascribed to the different distribution of phases along two directions due to the elongation of FMM domains along [01$\bar{1}$][11]. Therefore, the resistance of the heating branch in the [01$\bar{1}$] direction with an electric field applied would exhibit a much smaller increase than the one in the [100] direction. This explains the absence of the inverse hysteresis and positive colossal electroresistance in the [01$\bar{1}$] direction.

To further understand the key role of the preferential formation of elongated FMM domains induced by anisotropic strain-field in the observed abnormal percolative transport, the effect of magnetic field on the inverse hysteresis and positive colossal electroresistance was explored. We carry out transport measurements under joint applications of magnetic field and electric bias. If the preferential formation of elongated FMM domains indeed controls the percolative transport in the in-plane [100] direction, one can expect that applying a magnetic field along the [100] direction will result in an exchange of the transport behaviors of [100] and [01$\bar{1}$] since the magnetic field can force the FMM domains preferential seeding and growing along its direction. We do find this to be the case for applying a 5T magnetic field. Figure 6(a) and (b) display the temperature dependent resistance measured for in-plane [100] and [01$\bar{1}$] directions upon coactions of a 5T magnetic field along [100] and +10 kV/cm electric field along [011], respectively. One can find that the inverse hysteresis and the positive colossal electroresistance disappear in the [100] direction. Instead, a small positive electroresistance occurs in both cooling and heating branches accompanied with a negligible normal hysteresis. In contrast, the [01$\bar{1}$] direction does opposite and a pronounced inverse hysteresis appears e.g. ~ -5.7 K upon coactions of 5 T magnetic field and +10 kV/cm bias (indicated by orange arrows in Fig. 6(b)). A similar changeover of the percolative transport behaviors at [100] and [01$\bar{1}$] directions is also observed in the curves under the coactions of a 5 T magnetic field along [100] and a negative bias of −10 kV/cm along [011] (see the inset of Fig. 6(b)). An inverse hysteresis of ~ -3 K is identified for the [01$\bar{1}$] direction. These results unambiguously confirm that the anisotropic strain-field induced preferential formation of FMM domains is the main reason for the observed abnormal percolative behavior and positive colossal electroresistance in present phase separated PCSMO film.

In addition to the large anisotropic strain-field induced effects discussed above, another factor, polarization effect, may also contribute to the observed anisotropic colossal electroresistance since the bias field not only induces the dynamic strain effect but also poles the PMN-PT substrate[28,31,35]. It's known that the insulating regions of the film are transparent to the electric bias field, while the conducting regions are weakly affected since the electric field is screened out in the first few unit cells[36]. Therefore some field lines would terminate on FMM regions at the boundaries with COI regions. Thus the bias field could induce charges (holes or electrons) accumulation at the interface between COI and FMM regions, thereby moving the interface between these phases and changing the relative volume fraction of the COI and FMM regions[35]. In our case, the polarization effect induced by a positive bias field +10 kV/cm will accumulate holes at COI-FMM interfaces and push the interface to the side of FMM regions, resulting in an increase in resistance. Whereas the negative bias field will do the opposite. This leads to the relative low value of the positive colossal electroresistance under −10 kV/cm ($\sim$2130%) compared to the one under +10 kV/cm ($\sim$11460%). In another word, it is with the coactions of polarization and strong anisotropic strain effects that the positive colossal electroresistance behaves highly dependent on both orientation and bias polarity. In particular, it is upon the additive actions of the anisotropic strain-field and positive polarization-field that a colossal electroresistance as high as 11460% arises at [100] direction. On the contrary, small electroresistance and normal hysteresis appear along the [01$\bar{1}$] direction, which suggests that the polarization effect should dominate the per-

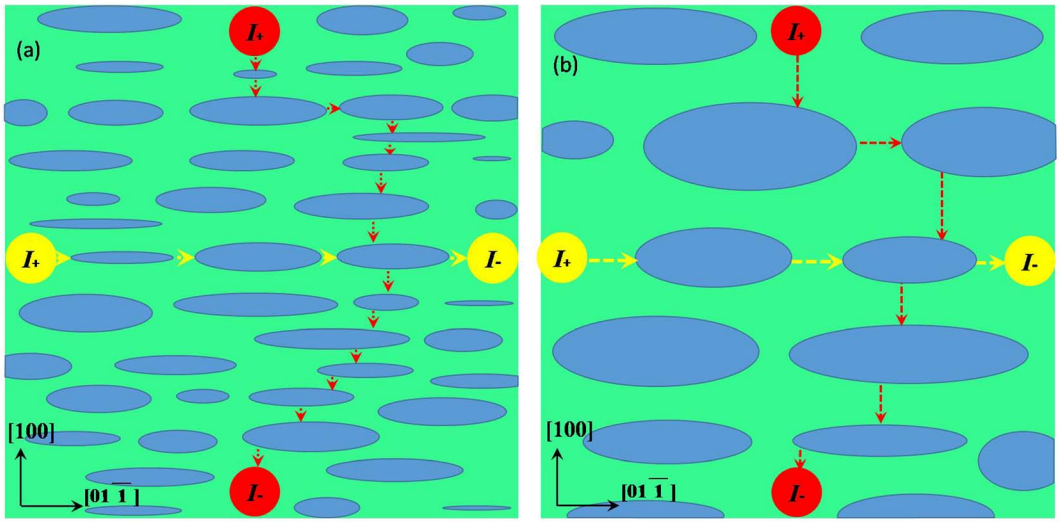

Figure 5 | Diagram of the percolative picture when the metal domains elongate along [01$\bar{1}$] due to the significant anisotropic strain-field induced by electric-field bias. (a) and (b) present the cooling and heating processes, respectively. Green regions represent insulating phases while blue ellipses indicate the elongated metallic domains. Yellow and red dotted lines with arrow indicate the possible current channel in insulating regions along two directions, respectively.

colative transport in the [01$\bar{1}$] direction. Actually, the large tensile strain in [01$\bar{1}$] would enhance the stabilities of long-range COO phases and leads to an increase in the resistance. This effect is against the one of the preferential formation of elongated FMM domains which results in a decrease in the resistance as discussed above. Such two opposite effects would largely cancel out each other and make polarization effect occupy the dominant role in the transport properties for [01$\bar{1}$] direction. Depending on the bias polarity, the dominant polarization effect would result in either an increase or a decrease in the resistance along the [01$\bar{1}$] direction (see Fig. 4(b) and its inset), similar to the case in $La_{0.7}Ca_{0.3}MnO_3$ system[24]. Note that the electroresistance upon heating process under −10 kV/cm shows a similar evolutionary trend compared to the one under +10 kV/cm, although most of its value are negative. This similarity reflects a competition between the polarization and tensile strain effect along the [01$\bar{1}$] direction[21,33,35].

Methods

The PCSMO thin films with 100 nm thickness were grown on (011)-PMN-PT single crystalline substrate by using pulsed laser deposition (PLD) technique. The commercial (011)-oriented slab of PMN-PT single crystal was chosen as substrate due to its excellent anisotropic converse piezoelectric effect, which provides an exceptional opportunity for dynamically generating a large in-plane anisotropic strain in the film epitaxially grown on it. A KrF excimer laser (248 nm) with a pulsed energy of 274 mJ and a repetition of 2 Hz was used. The substrate temperature was kept at 680°C and the oxygen pressure at 90 Pa during the deposition. After deposition, the films were cooled down to room temperature in 1 atm oxygen atmosphere. The crystalline structure and out-of-plane interplanar distance of both bulk and films were determined by means of x-ray diffraction (XRD) using Cu-Kα radiation. The bulk crystallizes in orthometric structure with space group of Pnma, and the pseudocubic lattice parameters were determined to be a=b=3.858 Å, c=3.854Å, respectively. X-ray reciprocal space maps (RSMs) around asymmetric reflections were collected by four-circle diffractometer (Bruker AXS D8-Discover) to determine epitaxial in-plane strains of thin films. The induced in-plane strains of films by electric bias were measured using a strain gauge (BX120-1AA) bonded on PCSMO films. Au layers were vapor deposited on both top and bottom sides of PCSMO/PMN-PT heterostructure as electrodes. A 20 MΩ resistor was presented in the circuit for protection (see the inset of Fig. 1(a)). The resistance of the PMN-PT, measured using a Keithley 6517A electrometer, was ~10 GΩ, and a negligible small leakage current was observed (less than 10 nA under a 10 KV/cm electric field). The strain-controlled percolative transport properties were measured using a superconducting quantum interference device (SQUID–VSM) with *in situ* electric fields applied across the PCSMO/PMN-PT structure. A Keithley 2600 was used as a constant-current source, providing a constant current of 1 μA. Meanwhile, the voltage was measured by using Keithley 2182. The electric bias on the (011)-PCSMO/PMN-PT heterostructures was provides by Keithley 6517A. The detailed circuit diagram is represented in the inset of

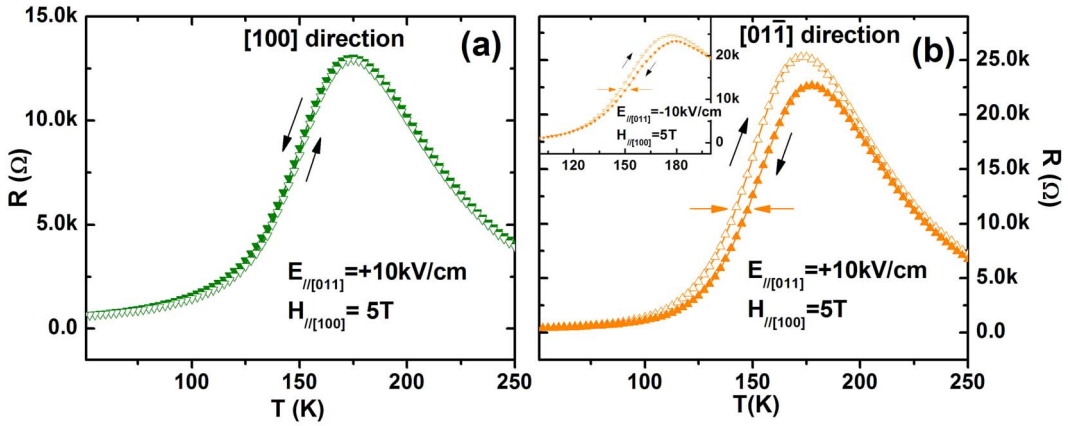

Figure 6 | Temperature dependent resistance for in-plane (a) [100] and (b) [01$\bar{1}$] directions upon joint applications of a 5T magnetic field along [100] and +10 kV/cm electric field along [011]. The inset of Fig. 6b shows the temperature dependent resistance for in-plane [01$\bar{1}$] direction upon joint applications of a 5T magnetic field along [100] and an negative electric bias of −10 kV/cm electric field along [011]. The black arrows indicate the warming/cooling paths while orange ones denote the hysteresis gap ΔT.

Fig. 1(a). To check the influence of the contact resistance in our two-probe measurements, four-probe method was further used to measure the temperature dependent resistance along [100] direction. No severe difference, especially for the abnormal inverse hysteresis and colossal electroresistance, was observed between the results deduced from two methods, indicating the influence of the contact resistance is trivial in our experiments and could be neglected (see section S2 in supplementary material).

1. Mathur, N. & Littlewood, P. Mesoscopic texture in manganites. *Phys. Today* **56**, 25–30 (2003).
2. Zhang, L. W., Israel, C., Biswas, A., Greene, R. L. & de Lozanne, A. Direct observation of percolation in a manganite thin Film. *Science* **298**, 805–807 (2002).
3. Tokunaga, M., Tokunaga, Y. & Tamegai, T. Imaging of percolative conduction paths and their breakdown in phase-separated $(La_{1-y}Pr_y)_{0.7}Ca_{0.3}MnO_3$ with y=0.7. *Phys. Rev. Lett.* **93**, 037203 (2004).
4. Dagotto, E., Hotta, T. & Moreo, A. Colossal magnetoresistant materials: the key role of phase separation. *Phys. Rep.* **344**, 1–153 (2001).
5. Burgy, J., Mayr, M., Martin-Mayor, V., Moreo, A. & Dagotto, E. Colossal effects in transition metal oxides caused by intrinsic inhomogeneities. *Phys. Rev. Lett.* **87**, 277202 (2001).
6. Ahn, K. H., Lookman, T. & Bishop, A. R. Strain-induced metal-insulator phase coexistence in perovskite manganites. *Nature (London)* **428**, 401–404 (2004).
7. Uehara, M., Mori, S., Chen, C. H. & Cheong, S. W. Percolative phase separation underlies colossal magnetoresistance in mixed-valent manganites. *Nature* **399**, 560–563 (1999).
8. Dong, S., Zhu, H., Wu, X. & Liu, J. M. Microscopic simulation of the percolation of manganites. *Appl. Phys. Lett.* **86**, 022501 (2005).
9. Moreo, A., Yunoki, S. & Dagotto, E. Solid state physics - Phase separation scenario for manganese oxides and related materials. *Science* **283**, 2034–2040 (1999).
10. Kimura, T., Tomioka, Y., Kumai, R., Okimoto, Y. & Tokura, Y. Diffuse phase transition and phase separation in Cr-doped $Nd_{1/2}Ca_{1/2}MnO_3$: A relaxor ferromagnet. *Phys. Rev. Lett.* **83**, 3940–3943 (1999).
11. Ward, T. Z. *et al.* Elastically driven anisotropic percolation in electronic phase-separated manganites. *Nature Phys.* **5**, 885–888 (2009).
12. Borges, R. P., Ott, F., Thomas, M. R., SKumryev, V. & Coey, J. M. D. Field-induced transition in the paramagnetic state of $(Sm_{0.65}Sr_{0.35})MnO_3$ associated with magnetic clusters. *Phys. Rev. B* **60**, 12847–12851 (1999).
13. Mahendiran, R., Raveau, B., Hervieu, M., Michel, C. & Maignan, A. Instability of metal-insulator transition against thermal cycling in phase separated Cr-doped manganites. *Phys. Rev. B* **64**, 064424 (2001).
14. De, K., Majumdar, S. & Giri, S. Memory effect and inverse thermal hysteresis in $La_{0.87}Mn_{0.98}Fe_{0.02}O_x$. *J. Appl. Phys.* **101**, 103909 (2007).
15. Markovich, V. *et al.* Inverse thermal hysteresis and Peculiar Transport Properties of $La_{0.9}MnO_{3-\delta}$ film. *J. Phys.: Conf. ser.* **200**, 052014 (2010).
16. Khomskii, D. & Khomskii, L. Fine mist versus large droplets in phase separated manganites. *Phys. Rev. B* **67**, 052406 (2003).
17. Burgy, J., Dagotto, E. & Mayr, M. Percolative transitions with first-order characteristics in the context of colossal magnetoresistance manganites. *Phys. Rev. B* **67**, 014410 (2003).
18. Burgy, J., Moreo, A. & Dagotto, E. Relevance of cooperative lattice effects and stress fields in phase-separation theories for CMR manganites. *Phys. Rev. Lett.* **92**, 097202 (2004).
19. Ward, T. Z. *et al.* Reemergent metal_insulator transitions in manganites exposed with spatial confinement. *Phys. Rev. Lett.* **100**, 247204 (2008).
20. Dhakal, T., Tosado, J. & Biswas, A. Effect of strain and electric field on the electronic soft matter in manganite thin films. *Phys. Rev. B* **75**, 092404 (2007).
21. Zhao, Y. Y. *et al.* Strain effect caused by substrates on phase separation and transport properties in $Pr_{0.7}(Ca_{0.8}Sr_{0.2})_{0.3}MnO_3$ thin films. *J. Appl. Phys.* **111**, 07D721 (2012).
22. Dho, J., Kim, Y. N., Hwang, Y. S., Kim, J. C. & Hur, N. H. Strain-induced magnetic stripe domains in $La_{0.7}Sr_{0.3}MnO_3$ thin films. *Appl. Phys. Lett.* **82**, 1434–1436 (2003).
23. Tomioka, Y. & Tokura, Y. Bicritical features of the metal-insulator transition in bandwidth-controlled manganites: Single crystals of $Pr_{1-x}(Ca_{1-y}Sr_y)_xMnO_3$. *Phys. Rev. B* **66**, 104416 (2002).
24. Jiang, T. *et al.* Coaction and distinguishment of converse piezoelectric and field effects in $La_{0.7}Ca_{0.3}MnO_3/SrTiO_3/0.68Pb(Mg_{1/3}Nb_{2/3})O_3$-$0.32PbTiO_3$ Heterostructures. *Appl. Phys. Lett.* **103**, 053504 (2013).
25. Thiele, C. *et al.* Voltage-controlled epitaxial strain in $La_{0.7}Sr_{0.3}MnO_3/Pb(Mg_{1/3}Nb_{2/3})O_3$-$PbTiO_3$(001) films. *Appl. Phys. Lett.* **87**, 262502 (2005).
26. Zhao, T. *et al.* Colossal magnetoresistive manganite-based ferroelectric field-effect transistor on Si. *Appl. Phys. Lett.* **84**, 750–752 (2004).
27. Shanthi, M., Lim, L. C., Rajan, K. K. & Jin, J. Complete sets of elastic, dielectric, and piezoelectric properties of flux-grown [011]-poled $Pb(Mg_{1/3}Nb_{2/3})O_3$-(28–32)% $PbTiO_3$ single crystals. *Appl. Phys. Lett.* **92**, 142906 (2008).
28. Wang, J., Hu, F. X., Chen, L., Sun, J. R. & Shen, B. G. The investigation of reversible strain and polarization effect in (011)-$La_{0.9}Ba_{0.1}MnO_3$ film using field effect configuration. *J. Appl. Phys.* **109**, 07d715 (2011).
29. Biegalski, M. D., Dörr, K., Kim, D. H. & Christen, H. M. Applying uniform reversible strain to epitaxial oxide films. *Appl. Phys. Lett.* **96**, 151905 (2010).
30. Thiele, C., Dorr, K., Bilani, O., Rodel, J. & Schultz. Influence of strain on the magnetization and magnetoelectric effect in $La_{0.7}A_{0.3}MnO_3$/PMN-PT(001) (A=Sr,Ca). *Phys. Rev. B* **75**, 054408 (2007).
31. Wang, J., Hu, F. X., Li, R. W., Sun, J. R. & Shen, B. G. Strong tensile strain induced charge/orbital ordering in (001)-$La_{7/8}Sr_{1/8}MnO_3$ thin film on $0.7Pb(Mg_{1/3}Nb_{2/3})O_3$–$0.3PbTiO_3$. *Appl. Phys. Lett.* **96**, 052501 (2010).
32. Sheng, Z. G., Gao, J. & Sun, Y. P. Coaction of electric field induced strain and polarization effects in $La_{0.7}Ca_{0.3}MnO_3$/PMN-PT structures. *Phys. Rev. B* **79**, 174437 (2009).
33. Mills, A. J., Littlewood, P. B. & Shraiman, B. I. Double exchange alone does not explain the resistivity of $La_{1-x}Sr_xMnO_3$. *Phys. Rev. Lett.* **74**, 5144–5147 (1995).
34. Stauffer, D. & Aharoni, A. [Conductivity and related properties]. *Introduction to Percolation Theory*. [89–108] (Taylor & Francis, New York, 1994).
35. Wu, T. *et al.* Electroresistance and electronic phase separation in mixed-valent manganites. *Phys. Rev. Lett.* **86**, 5998–6001 (2001).
36. Hu, J. M., Nan, C. W. & Chen, L. Q. Size-dependent electric voltage controlled magnetic anisotropy in multiferroic heterostructures: interface-charge and strain comediated magnetoelectric coupling. *Phys. Rev. B* **83**, 134408 (2011).

Acknowledgments

This work was supported by the National Basic Research of China (Grant Nos. 2012CB933001, 2014CB643702 and 2013CB921700), the National Natural Science Foundation of China with Grant Nos. 11174345, 11474341, 11074286 and 11374348.

Author contributions

J.W. and F.X.H. planned and supervised the experiments. Y.Y.Z. prepared the samples and carried out X-ray diffraction and magnetic transport measurements. H.R.Z. and Y.Y.Z. performed the experiments of reciprocal space maps. Y.Y.Z., H.K. and L.F.B. performed the dynamic strain measurements and analyzed the strain data. Y.Z. Performed the experiments of Lorentz TEM. Y.L., S.H.W., R.R.W. and M.Z. assisted in the measurements of magnetic and transport properties. J.W. and F.X.H. prepared the manuscript and refined the paper. J.R.S. and B.G.S. made scientific comment on the manuscript. All authors discussed the results and contributed to the refinement of the paper.

Additional information

Supplementary information accompanies this paper at http://www.nature.com/scientificreports

Competing financial interests: The authors declare no competing financial interests.

How to cite this article: Zhao, Y.-Y. *et al.* Abnormal percolative transport and colossal electroresistance induced by anisotropic strain in (011)-$Pr_{0.7}(Ca_{0.6}Sr_{0.4})_{0.3}MnO_3$/PMN-PT heterostructure. *Sci. Rep.* **4**, 7075; DOI:10.1038/srep07075 (2014).